Published in final edited form as:
Nat Med. 2013 October ; 19(10): 1338–1344. doi:10.1038/nm.3324.

Tracking adipogenesis during white adipose tissue development, expansion and regeneration

Qiong A Wang[1], **Caroline Tao**[1], **Rana K Gupta**[1], and **Philipp E Scherer**[1,2]

[1]Touchstone Diabetes Center, Department of Internal Medicine, The University of Texas Southwestern Medical Center, Dallas, Texas, USA

[2]Department of Cell Biology, The University of Texas Southwestern Medical Center, Dallas, Texas, USA

Abstract

White adipose tissue displays high plasticity. We developed a system for the inducible, permanent labeling of mature adipocytes that we called the AdipoChaser mouse. We monitored adipogenesis during development, high-fat diet (HFD) feeding and cold exposure. During cold-induced 'browning' of subcutaneous fat, most 'beige' adipocytes stem from *de novo*–differentiated adipocytes. During HFD feeding, epididymal fat initiates adipogenesis after 4 weeks, whereas subcutaneous fat undergoes hypertrophy for a period of up to 12 weeks. Gonadal fat develops postnatally, whereas subcutaneous fat develops between embryonic days 14 and 18. Our results highlight the extensive differences in adipogenic potential in various fat depots.

The ongoing obesity epidemic in both the western and developing worlds has raised awareness of the complex physiology of adipose tissue. It is widely appreciated that anatomically distinct adipose tissues differ substantially in their contributions to energy balance and nutrient homeostasis. Adipose tissue distribution is a strong predictor of the occurrence of the metabolic syndrome in the context of obesity. Obese individuals who preferentially expand visceral adipose tissue are at a greater risk for diabetes and cardiovascular disease than are equally obese individuals who store excess energy in subcutaneous adipose tissue[1–3]. In fact, the expansion of subcutaneous adipose tissue can be potently protective against metabolic complications of HFD feeding[4,5].

The mechanism by which individual adipose depots expand may also be a critical determinant of the metabolic syndrome in obesity. In principle, adipose tissue expansion can occur through an enlargement in adipocyte size (hypertrophy) or an increase in adipocyte numbers (hyperplasia). Differentiated adipocytes are post-mitotic; therefore, hyperplasia represents an increase in *de novo* adipocyte formation (adipogenesis). Adipocyte

Correspondence should be addressed to P.E.S. (philipp.scherer@utsouthwestern.edu).

Author Contributions: Q.A.W. designed and performed the experiments and wrote the manuscript. C.T. assisted with mouse experiments. R.K.G. and P.E.S. conceptualized and designed the study and wrote the manuscript.

Competing Financial Interests: The authors declare no competing financial interests.

hypertrophy is closely linked to adipose dysfunction: this pathological expansion of white adipose tissue (WAT) is a major component of the metabolic syndrome in obese individuals[6]. Both adipocyte hypertrophy and hyperplasia contribute to adipose tissue expansion during HFD challenge[6,7]. However, it remains under debate whether adipogenesis is induced immediately after HFD exposure and whether there are depot differences in response to HFD with respect to adipogenesis[8,9]. Recent studies have highlighted the critical role of *in vivo* adipogenesis as it relates to key adipogenic precursor cells[10–15].

WAT is known to have high physiological plasticity. Exposure to cold or pharmacological treatment with β-adrenergic receptor (β3) agonists that enhance lipolysis in adipocytes triggers the appearance of a subset of potentially beneficial adipocytes within the WAT that are positive for uncoupling protein 1 (UCP1) and share additional characteristics with brown adipocytes[16–19]. Unlike classic brown adipocytes, these 'brown-like' fat cells, termed beige adipocytes, do not derive from precursors that are positive for myogenic factor 5 (Myf5)[20]. Recent studies have suggested that in subcutaneous adipose tissue, newly induced brown adipocytes are not associated with precursor proliferation[21] and may arise from the transdifferentiation of existing white adipocytes[22–24]. Conversely, others have found that there is a $CD137^+$ precursor cell population that is at rest in subcutaneous adipose tissue and can be activated to differentiate into brown adipocytes after appropriate stimulation[15]. However, to date, there has been no direct evidence found for the unambiguous lineage of these beige adipocytes. Leptin reporter mice have been valuable in identifying early waves of adipogenesis occurring developmentally[25]; however, inducible lineage-tracing mouse models to examine adipogenesis are still lacking.

To better understand the dynamics of adipocytes in different fat depots, we developed a doxycycline-inducible, mature adipocyte–specific tracing system that we refer to as the AdipoChaser mouse. We are thus in a unique position to answer the questions outlined above *in vivo* with a high degree of temporal resolution. By using a pulse-chase system that allows us to label all pre-existing mature adipocytes, we uncovered the differential adipogenic capacity of epididymal and subcutaneous adipose tissue during HFD-induced adipose tissue expansion. Our studies also offer insights into the unresolved issue of whether brown-like fat cells induced by cold exposure or β3 agonist treatment in subcutaneous adipose tissue arise from existing mature adipocytes or derive from *de novo* differentiation. Most notably, we found that cold exposure or β3 agonist stimulation induces massive white adipogenesis in epididymal adipose tissue. In addition, our labeling system allowed us to determine the exact developmental time frame of adipocyte differentiation in gonadal and subcutaneous adipose tissue.

Results

The contribution of hyperplasia to adipose tissue expansion

In order to study the fate of mature adipocytes under different metabolic challenges, we developed the AdipoChaser mouse, which is an inducible adipocyte-tagging system. This model is a combination of three transgenic lines that we and other labs have generated: the adiponectin promoter-driven tetracycline-on (Tet-on) transcription factor rtTA (*adiponectinP-rtTA*)[26], a Tet-responsive Cre (*TRE-cre*) line that can be activated by rtTA in

the presence of doxycycline[27] and a transgenic line carrying *Rosa26* promoter–driven *loxP-stop-loxP*–β-galactosidase (*Rosa26-loxP-stop-loxP-lacZ*)[28] (Fig. 1a). In the absence of doxycycline, there was no LacZ expression in mature adipocytes. After treatment with doxycycline, rtTA activates the *TRE* promoter to induce *cre* expression. Cre protein subsequently eliminates the floxed transcriptional stop cassette and permanently turns on LacZ expression in all mature adipocytes present during doxycycline exposure. Cells can be stained blue with an appropriate β-galactosidase (β-gal) substrate. After 2 weeks of doxycycline treatment, all adipocytes in both the epididymal and subcutaneous white adipose tissues (eWAT and sWAT, respectively) of the triple transgenic (AdipoChaser) mice were uniformly labeled blue (Fig. 1b,c), reflecting the presence of β-gal activity. Other cell types, such as endothelial cells in the subcutaneous adipose tissue, were not labeled (Fig. 1c). We also used β-gal substrate to stain adipocytes from control (containing only *TRE-cre* and *Rosa26-loxP*-stop-*loxP-lacZ*) mice treated with doxycycline and adipocytes from AdipoChaser mice kept on chow diet; none of these stainings showed a β-gal signal (Fig. 1b,c). We next tested the washout period of doxycycline in mice. We kept AdipoChaser mice on doxycycline diet for 7 d and then switched them to chow diet without doxycycline for time periods ranging from overnight to up to 3 d before analyzing them. Real-time quantitative PCR (qPCR) results showed that each group of AdipoChaser mice had a similar level of rtTA expression in subcutaneous adipose tissue (Supplementary Fig. 1). Cre expression levels in AdipoChaser mice after 3, 2 or 1 d or overnight doxycycline withdrawal were comparable to the expression levels in AdipoChaser mice kept on chow diet without doxycycline and were much lower than those in AdipoChaser mice treated continuously in the presence of doxycycline (Supplementary Fig. 1). During the same time course, AdipoChaser mice had similar levels of LacZ expression throughout the doxycycline withdrawal periods that were much higher than those in mice never treated with doxycycline (Supplementary Fig. 1). These results show that an overnight withdrawal is sufficient to completely wash out doxycycline in mice.

Using this system, we initially focused on the rate of appearance of *de novo*–differentiated adipocytes during HFD challenge. We first gave AdipoChaser mice doxycycline diet for 7 d to ensure uniform and permanent labeling of mature adipocytes with LacZ, which we followed with 3 d of chow diet to ensure that the doxycycline was fully washed out. Thereafter, we fed the mice either chow or HFD (60% of calories from fat) for various lengths of time. HFD feeding for 12 weeks increased the body weight of AdipoChaser mice by 51% ($P < 0.001$) as compared to the basal body weight of the mice before beginning the HFD, whereas AdipoChaser mice kept on chow had only a 15% increase in body weight ($P < 0.001$) (Supplementary Fig. 2a). The weights of epididymal adipose tissue and subcutaneous adipose tissue of 12-week HFD-fed AdipoChaser mice were increased by 84% ($P < 0.001$) and 163% ($P < 0.001$), respectively, compared to age-matched AdipoChaser mice kept on chow diet (Supplementary Fig. 2b,c). AdipoChaser mice fed with chow diet showed no new adipogenesis, as determined by the fact that all fat depots displayed nearly 100% positive β-gal staining in adipocytes, even at up to 59 d after doxycycline treatment (Fig. 2). Thus, extremely low levels of adipogenesis were present in both epididymal and subcutaneous adipose tissues (Fig. 2a,c). After HFD feeding for 7 d, adipocytes in both the epididymal and subcutaneous adipose tissues still showed nearly 100% LacZ labeling with

no obvious morphological changes (Fig. 2b,d). When we kept mice on HFD for 35 d, the average size of the adipocytes in both depots increased markedly, reflecting a high capacity for cell hypertrophy (Fig. 2b,d). After 56 or 89 d of HFD feeding, epididymal adipose tissue showed a high adipogenesis rate, as determined by a large number of β-gal–negative cells (Fig. 2b); in contrast, the subcutaneous adipose depot maintained a relatively low rate of adipogenesis, as evidenced by nearly 100% LacZ labeling (Fig. 2d). These observations indicate that HFD-induced adipose tissue expansion is contributed mainly by hypertrophy during the first month of HFD. After prolonged HFD exposure (i.e., longer than 1 month), a wave of adipogenesis is preferentially initiated in epididymal adipose tissue, whereas only negligible levels of adipogenesis occur in subcutaneous adipose tissue depots (Fig. 2e). These experiments reveal the surprising property of subcutaneous adipose tissue to use *de novo* adipogenesis only minimally as a mechanism to cope with chronic caloric excess.

Beige adipocytes arise by *de novo* adipogenesis

It is not clear whether the beige cells that are induced by cold exposure or β3 agonist treatment arise through transdifferentiation of existing white adipocytes or by *de novo* adipogenesis from a subgroup of precursor cells. We therefore studied newly developed beige adipocytes within subcutaneous adipose tissue under those conditions. We pretreated AdipoChaser mice with doxycycline diet for 7 d to ensure uniform, permanent expression of LacZ in mature adipocytes, which we followed with 3 d of chow diet to wash out the doxycycline. Overnight cold exposure in doxycycline-pretreated mice on a chow diet showed clusters of cells within the subcutaneous adipose tissue that were smaller than normal white adipocytes and that displayed negative β-gal staining (Fig. 3a). Three days of cold exposure induced massive browning of subcutaneous adipose tissue, with the AdipoChaser mice showing large areas of beige fat cells with multiple small lipid droplets, and most of these tissues had negative β-gal staining (Fig. 3a). These new adipocytes were preserved for at least 7 d in the subcutaneous adipose tissue after we switched the mice back to room temperature (Fig. 3a). In mice that we kept on doxycycline diet throughout the cold exposure, ∼100% of the beige adipocytes showed LacZ-positive signals, demonstrating that these newly emerging cells can indeed be labeled if the mouse remains exposed to doxycycline during cold exposure (Fig. 3b). We observed similar results in the β3 agonist–treated mice: most of the newly generated beige adipocytes in these mice were negative for β-gal staining (Fig. 3c).

Immunofluorescence staining demonstrated that LacZ-negative cells that formed in the subcutaneous adipose tissue of AdipoChaser mice were positive for the lipid droplet–specific marker perilipin, Ucp1 and the beige cell marker Cbp/p300-interacting transactivator with Glu/Asp-rich C-terminal domain, 1 (Cited1)[29], whereas the LacZ-positive blue adipocytes were positive for perilipin only (Fig. 3d–f). These results indicate that after cold exposure or β3 agonist treatment, most beige adipocytes are induced by *de novo* differentiation from cell populations other than existing mature adipocytes (i.e., $Cited1^{+}Cd137^{+}$ beige precursors) rather than by a transdifferentiating mature white adipocyte (Fig. 3g). Beige cells can also revert to a white adipocyte phenotype, as has been recently reported[30] (Fig. 3g).

Cold-induced adipogenesis in epididymal adipose tissue

Previous studies have shown that the appearance of brown-like cells is observed mainly in subcutaneous adipose tissue. Very few of these newly emerging cells can be detected in the visceral fat[20]. Notably, after cold exposure during as short a time period as overnight, epididymal adipose tissue of mice pretreated with doxycycline on a chow diet showed numerous β-gal–negative cells (Fig. 4a and Supplementary Fig. 3). Unlike beige adipocytes, these new cells were larger in size and had only a single large lipid droplet. Three days of cold exposure further increased the number of β-gal–negative cells in epididymal adipose tissue (Fig. 4a), and the newly generated adipocytes remained present even after we switched the mice back to room temperature (Fig. 4a). As a control, we used mice kept on a doxycycline diet throughout cold exposure and found that every adipocyte in these mice showed a LacZ-positive signal, demonstrating that these newly emerging cells in epididymal adipose tissue can be labeled if the mouse remains exposed to doxycycline during cold exposure (Fig. 4b). Similarly, in the β3 agonist–treated mice, β-gal–negative white adipocytes appeared in epididymal adipose tissue (Fig. 4c). In order to provide further evidence that adipogenesis in the epididymal adipose tissue is triggered after cold exposure, we isolated RNA from the epididymal adipose tissue of mice that we either left unexposed or exposed to cold for 3 d for qPCR analysis of *lacZ* expression and other adipocyte markers. Compared to mice kept at room temperature, mice that were exposed to cold had decreased *lacZ* expression in epididymal adipose tissue (by 53%, $P < 0.05$), with no change in *rtTA* expression or that of other adipocytes markers, such as *Adipoq* (adiponectin) or *Pparg2* (peroxisome proliferator-activated receptor γ2) (Fig. 4d). Immunofluorescence staining showed that these β-gal–negative cells were perilipin positive but Ucp1 negative (Fig. 4e,f). These cells were therefore live cells that had a gene expression pattern consistent with that of classic white adipocytes.

We next wanted to determine whether cold exposure increases the tissue mass of epididymal adipose tissue. Three days of cold exposure slightly but significantly decreased the body weight of wild-type mice (by 6%, $P < 0.05$) (Supplementary Fig. 4a). The weights of both epididymal and subcutaneous adipose tissues were decreased after cold exposure (by 32%, $P < 0.05$) and 36% ($P < 0.001$), respectively) compared to mice kept at room temperature (Supplementary Fig. 4b). This observation indicates that despite ongoing adipogenesis in epididymal adipose tissue during cold exposure, epididymal adipose tissue mass does not increase overall but instead decreases. Taken together, our data provide strong evidence that widespread browning occurs in subcutaneous adipose tissue through *de novo* adipogenesis during cold exposure or β3 agonist stimulation. In parallel, there is a substantial amount of *de novo* adipogenesis of white adipocytes that occurs under these conditions, primarily in epididymal adipose tissue (Fig. 4g).

Adipogenesis during development

Having examined the behavior of fat pads under different conditions in adult mice, we then studied commitment to the adipocyte lineage during development. In order to label adipocytes during embryogenesis, we exposed AdipoChaser mice to doxycycline diet for various time periods during pregnancy and analyzed the offspring at postnatal day (P) 28 or 56 (Fig. 5). In gonadal adipose tissue, both male and female mice whose mothers were on

doxycycline during embryonic day (E) 9–16 or E19–P4 showed very few LacZ-positive cells once the mice were 28 days old (Fig. 5a). In AdipoChaser mice whose mothers were on doxycycline until P10, most of the adipocytes in the gonadal adipose tissue were LacZ negative on P28 (Fig. 5a and Supplementary Fig. 5) or P56 (Fig. 5c). For mice whose mothers were on doxycycline during the period E19–P20, large areas of the adipocytes in the gonadal adipose tissue were LacZ positive when the mice were 28 days old, but there were also numerous adipocytes that developed after P20, as judged by negative LacZ staining (Fig. 5a). These data show that gonadal adipocytes undergo differentiation postnatally for the most part, and this differentiation happens gradually over a relatively long period of time after birth.

In contrast, subcutaneous adipose tissue showed a rather distinct pattern. None of the male AdipoChaser mice whose mothers were on doxycycline during E7–E14 showed any LacZ-positive adipocytes when examined on day 28, whereas female AdipoChaser mice under the same conditions showed a few (<5%) LacZ-positive adipocytes (Fig. 5b). However, adipocytes in subcutaneous tissue of mice whose mothers were on doxycycline during E9–E16 showed a heterogeneous pattern of LacZ-positive cells, with some regions carrying more than 90%, and other regions displaying less than 50%, LacZ-positive cells (Fig. 5b). AdipoChaser mice whose mothers were on doxycycline treatment during E9–E18 or E19–P10 showed nearly 100% LacZ-positive cells in subcutaneous adipose tissue (Fig. 5b and Supplementary Fig. 5). These observations indicate that for subcutaneous adipocytes, adipocyte commitment and differentiation are initiated during E14–E18 in both genders. Large areas of the subcutaneous adipose tissue were still very small and lacked mature adipocyte morphology in the perinatal phase (28 d) (Fig. 5b). When mice whose mothers were on doxycycline during E19–P10 were 56 days old, adipocytes in the subcutaneous adipose tissue in both genders remained LacZ positive and were fully differentiated with relatively even cell sizes and single lipid droplets (Fig. 5d). Notably, there were also some LacZ-positive nonadipocytes around the vascular structure in the subcutaneous adipose tissue (Fig. 5b), even in mice whose mothers were on doxycycline during E7–E14 (Fig. 5b). These results suggest that, unlike gonadal adipocytes, subcutaneous adipocytes are committed and differentiated much earlier during embryogenesis. Although subcutaneous adipose tissue takes more time for complete differentiation, the number of adipocytes remains very stable postnatally (Fig. 5e).

Discussion

Assessments of *in vivo* adipogenesis have relied on measurements of cells size or BrdU incorporation into adipocytes[8,9]. The underlying assumption in using such methods is that adipocyte size reflects the age of the adipocyte and that preadipocyte proliferation precedes adipogenesis. Here we applied a genetic model that permitted the uniform labeling of mature adipocytes in WAT. By using this model, we found that the rate of white adipogenesis in both epididymal and subcutaneous adipose tissue in adult mice was very low when the animals were maintained on a chow diet. This is consistent with human studies that demonstrated previously that only about 10% of adipocytes are renewed annually in adults[31]. During the early stages of HFD exposure (i.e., within about 1 month of beginning the diet), we observed that hypertrophy was the main phenomenon contributing to adipose

tissue expansion in both epididymal and subcutaneous adipose tissues. At more prolonged stages of HFD exposure (i.e., 2 months), a high capacity for adipogenesis was apparent in gonadal adipose tissues. In contrast, subcutaneous adipose tissues maintained an extremely low rate of adipogenesis, even after 2 months of HFD exposure. These results highlight that the adipogenesis rates of different fat pads differ extensively. This helps to better explain phenomena related to prolonged HFD exposure. It also underscores the fact that phenomena related to the isolation of stromal vascular fractions (SVFs) from various fat pads and their ability to *in vitro* differentiate do not relate to their *in vivo* capacity to undergo adipogenesis. In fact, cultures of stromal vascular cells derived from subcutaneous fat regions readily give rise to adipocytes *in vitro*; however, subcutaneous adipogenesis *in vivo* seems to be limited, at least in the male mice that we analyzed here.

Brown adipocytes have the potential to be metabolically beneficial, especially for obese individuals, as they have the potential for enhanced energy expenditure after proper stimulation. Although we cannot exclude that there is some degree of transdifferentiation, our findings demonstrate that most of the newly emerging beige adipocytes that appear in subcutaneous depots are not derived from existing white adipocytes. They therefore must derive from a precursor cell type that undergoes differentiation rather than from the transdifferentiation of existing adipocytes. This is consistent with a recent report that demonstrated that brown-like adipocytes derive from $Cd137^+$ cells[15]. BrdU incorporation into cells has been widely used as an indicator of adipogenesis. However, the lack of BrdU incorporation only highlights that there is no cell-proliferative step in subcutaneous adipose tissue[21]. If beige adipocytes derive from resting precursor cells[15] with very limited proliferation, the newly formed cells will also be BrdU negative.

Our experiments reveal another interesting phenomenon that is difficult to detect in the absence of the type of labeling techniques that we used here. We found that cold exposure or β3 agonist stimulation induced widespread white adipocyte differentiation in the epididymal adipose tissue, a phenomenon that is markedly different from the browning effect seen in subcutaneous adipose tissues under these conditions. The current consensus in the field views epididymal adipose tissue as relatively nonresponsive to adrenergic stimulation, and our data support this view when we compare the potential for browning of the epididymal depot with that of the subcutaneous depots. However, our LacZ pulse and chase experiments revealed that epididymal adipose tissue is potently responsive to cold stimuli. This is an interesting phenomenon, and one previous report has suggested that this may be the case. Miller and Faust reported in 1982 that maintaining rats for 24 weeks in the cold was associated with an increase in adipocyte numbers selectively in the epididymal adipose tissue, a phenomenon they did not observe in any other fat pads[32]. They contrast this development to HFD-induced changes that induce proliferative events in retroperitoneal but not epididymal adipose tissue. Our findings suggest that this cold-induced adipogenesis in epididymal adipose tissue is a very fast process, occurring within a few days of cold exposure.

In recent years, a number of studies have focused on the characteristics of fat progenitor cells. Mesenchymal stem cells isolated from adipose tissue have been shown to have the potential to differentiate into various cell types, including adipocytes[33]. It is known that

adipocyte precursor stem cells are present in the pool of stromal vascular cells (the SVF) of adipose tissue. These cells can be differentiated into mature adipocytes both *in vitro* and *in vivo*[11]. Similarly to Ppar-γ, zinc finger protein 423 (Zfp423) has been discovered to be a marker of committed preadipocytes[12,13]. Expression analyses of PPAR-γ or Zfp423 have revealed that adipogenic precursors are located around the vascular wall of adipose tissue[10,13]. However, it is still unknown whether the progenitor cells that give rise to white adipocytes during the normal development of new adipose tissue share the same characteristics and respond to the same stimuli as their counterparts that undergo adipose tissue adipogenesis and regeneration during adulthood and aging. It is also not understood how many features there are in common between visceral and subcutaneous precursors. It has been shown that some pad-specific characteristics are preserved after isolation and *in vitro* differentiation of these cells[34]. Our lineagetracing studies showed that epididymal adipose tissue has a relatively high potential to undergo adipogenesis under various environmental challenges, such as HFD challenge or cold exposure. In addition, the time frame of gonadal adipose tissue development is completely different from that of subcutaneous adipose tissue. It is therefore entirely possible that these two depots may not share the same progenitors. Alternatively, precursors from these two depots either do not respond to the same stimuli to differentiate or are differentially exposed to those signals because of differential spatial organization. It is noteworthy that the SVF from subcutaneous adipose tissues differentiates more robustly and readily *in vitro* than the SVF from epididymal adipose tissue[35–37]. This has led many to believe that this observation may underlie the physiological basis of why subcutaneous WAT in humans seems to expand predominantly through hyperplasia[35–37]. However, the data here clearly indicate that in mice, epididymal adipose tissue is more prone to undergoing differentiation than is subcutaneous adipose tissue. Understanding the underlying mechanisms for these phenomena is more than an academic exercise. The location of adipose tissue accumulation is of paramount importance with respect to clinical readouts for the metabolic syndrome in the clinic[38,39]. We have published several preclinical models that highlight the protective effects that are associated with subcutaneous adipose tissue expansion[4,5]. The *in vitro* studies highlight the potential for subcutaneous adipogenesis. However, under most conditions, subcutaneous adipogenesis is not activated *in vivo*. This highlights the existence of a critical ‘switch’ that must be activated *in vivo* to steer local events away from the hypertrophic growth of existing adipocytes and initiate the more beneficial cascade that leads to increases in the number of adipocytes.

In summary, by using an inducible mature adipocyte lineage–tracing system, the AdipoChaser mouse, we characterized the differentiation of adipocytes in various adipose tissues during development and explored the dynamics of these adipose tissues under various physiological challenges. The variation of timing and rates of adipogenesis in different adipose tissues highlight the unique characteristics of the depots that should each be treated as a separate ‘miniorgan’. The hope is that we will develop approaches in the future that allow us to manipulate these fat pads in a depot-specific fashion.

Methods

Methods and any associated references are available in the online version of the paper.

Note: Any Supplementary Information and Source Data files are available in the online version of the paper.

Online Methods

Mice

Mice were maintained on a 12-h dark, 12-h light cycle and were housed in groups of three to five with unlimited access to water and food (chow: number 5058, lab diet; HFD: number D1292, Research diet; doxycycline diet (600 mg per kg diet): S4107, Bio-Serv, as indicated in the individual experiments). The Institutional Animal Care and Use Committee of the University of Texas Southwestern Medical Center, Dallas, approved all animal experiments. All mice were on the C57BL/6J background. The *adnP-rtTA* mouse was generated as previously described[26]. *TRE-cre* and *Rosa26-loxP*-stop-*loxP-lacZ* lines were obtained from Jackson Laboratories. For lineage-tracing studies, *adnP-rtTA* mice were intercrossed to the *TRE-cre* and *Rosa26-loxP*-stop-*loxP-lacZ* strains, and we refer to these triple transgenic mice as AdipoChaser mice.

β-gal staining of adipose tissue

Mice at 10–12 weeks of age were anesthetized and perfused with 0.2% glutaraldehyde in PBS. Fat depots of interest were removed into a 6-cm cell culture dish containing 0.2% glutaraldehyde and cut into small slices. The sliced tissue was washed with rinse buffer (100 mM sodium phosphate, 2 mM $MgCl_2$, 0.01% sodium deoxycholate and 0.02% NP-40) three times and then soaked in β-gal staining buffer (5 mM potassium ferricyanide, 5 mM potassium ferrocyanide and 1 mg ml^{-1} β-gal substrate in rinse buffer) for 48 h at room temperature with mild shaking. After developing the β-gal stain, the sliced tissue was moved into 10% formalin overnight for post-fixation. The post-fixed tissue was processed with a standard paraffin tissue-embedding protocol to produce sections. After paraffin embedding and sectioning, tissues were counterstained with nuclear fast red. The staining was imaged using a Coolscope microscope (Nikon). Each β-gal stain image is a representative image from $n = 2–3$ mice out of two to three independent experiments.

Cold exposure and β3 agonist treatment

For cold exposure experiments, 10- to 11-week-old male AdipoChaser mice were kept in individual cages and maintained on chow diet or doxycycline diet for 3 d before cold exposure. During cold exposure, mice were kept on chow diet or doxycycline diet in individual cages and housed in a cold cabinet (6 °C) for the indicated times with free access to food and water. Alternatively, 10-week-old mice were treated with β3 agonist (CL-316243, Sigma) at 1 mg per kg body weight daily by intraperitoneal injections for 7 d while on a chow diet.

Immunofluorescence staining

Adipose tissues were prestained with β-gal solution and fixed in 10% PBS-buffered formalin overnight. Formalin-fixed, paraffin-embedded sections were blocked in PBS plus Tween-20 (PBST) with 5% BSA. The primary antibodies used were to Ucp1 (ab23841, Abcam, 1:200), perilipin (1:200) (a kind gift of A. Greenberg, Tufts University) and Cited1 (ab15096,

Abcam, 1:300); the secondary antibody used was Alexa Fluor 488 goat antibody to rabbit IgG (H+L) (A-11008, Invitrogen, 1:200)). Slides were counterstained with DAPI. Images were acquired using an AxioObserver epifluorescence microscope (Zeiss).

Quantitative real-time RT-PCR

Total RNA from mouse tissues was isolated using the RNeasy Mini Kit (QIAGEN). First-strand cDNA was synthesized with M-MLV reverse transcriptase and random hexamer primers (Invitrogen) from 1 μg of RNA. Real-time quantitative PCR was done with the SYBR Green PCR system (Applied Biosystems) using *Gapdh* as an internal control for normalization. The primers used were as follows (given as forward and reverse, respectively): *rtTA* (5′-AGTCATTCCGCTGTGCTCTC-3′, 5′-GCTCCTGTTCCTCCAATACG-3′), *lacZ* (5′-ACTATCCCGACCGCCT TACT-3′, 5′-GTGGGCCATAATTCAATTCG-3′), *Adipoq* (5′-GTTGCAA GCTCTCCTGTTCC-3′, 5′-ATCCAACCTGCACAAGTTCC-3′), *Pparg2* (5′-TGCACTGCCTATGAGCACTT-3′, 5′-AACCATTGGGTCAGCTCT TG-3′), *Gapdh* (5′-AACTTTGGCATTGTGGAAGG-3′, 5′-ACACATTG GGGGTAGGAACA-3′).

Statistical analyses

Data are presented as the means ± s.e.m. Differences were analyzed by unpaired two-tailed *t* test between two groups. There was no randomization or blinding during data analysis. No statistical method was used to predetermine sample size.

Supplementary Material

Refer to Web version on PubMed Central for supplementary material.

Acknowledgments

We thank the University of Texas Southwestern Histology Core for assistance in embedding and processing tissue samples, especially J.M. Shelton for suggestions and discussions on the protocol of LacZ staining of adipose tissues. We also thank A.S. Greenberg from Tufts University for providing perilipin antibody. This study was supported by US National Institutes of Health (NIH) grants R01-DK55758, P01-DK088761 and R01-DK099110 (P.E.S.). Q.A.W. is supported by a postdoctoral fellowship from the American Diabetes Association (7-11-MN-47). R.K.G. is supported by NIH grants K01-DK090120-02 and R03-DK099428 and the Searle Scholars Program (Chicago, Illinois).

References

1. Abate N, Garg A, Peshock RM, Stray-Gundersen J, Grundy SM. Relationships of generalized and regional adiposity to insulin sensitivity in men. J Clin Invest. 1995; 96:88–98. [PubMed: 7615840]
2. Miyazaki Y, DeFronzo R. Visceral fat dominant distribution in male type 2 diabetic patients is closely related to hepatic insulin resistance, irrespective of body type. Cardiovasc Diabetol. 2009; 8:44. [PubMed: 19656356]
3. McLaughlin T, Lamendola C, Liu A, Abbasi F. Preferential fat deposition in subcutaneous versus visceral depots is associated with insulin sensitivity. J Clin Endocrinol Metab. 2011; 96:E1756–E1760. [PubMed: 21865361]
4. Kim JY, et al. Obesity-associated improvements in metabolic profile through expansion of adipose tissue. J Clin Invest. 2007; 117:2621–2637. [PubMed: 17717599]

5. Kusminski CM, et al. MitoNEET-driven alterations in adipocyte mitochondrial activity reveal a crucial adaptive process that preserves insulin sensitivity in obesity. Nat Med. 2012; 18:1539–1549. [PubMed: 22961109]
6. Sun K, Kusminski CM, Scherer PE. Adipose tissue remodeling and obesity. J Clin Invest. 2011; 121:2094–2101. [PubMed: 21633177]
7. Prins JB, O'Rahilly S. Regulation of adipose cell number in man. Clin Sci (Lond). 1997; 92:3–11. [PubMed: 9038586]
8. Joe AWB, Yi L, Even Y, Vogl AW, Rossi FMV. Depot-specific differences in adipogenic progenitor abundance and proliferative response to high-fat diet. Stem Cells. 2009; 27:2563–2570. [PubMed: 19658193]
9. Jo J, et al. Hypertrophy and/or hyperplasia: dynamics of adipose tissue growth. PLOS Comput Biol. 2009; 5:e1000324. [PubMed: 19325873]
10. Tang W, et al. White fat progenitor cells reside in the adipose vasculature. Science. 2008; 322:583–586. [PubMed: 18801968]
11. Rodeheffer MS, Birsoy Kv, Friedman JM. Identifcation of white adipocyte progenitor cells *in vivo*. Cell. 2008; 135:240–249. [PubMed: 18835024]
12. Gupta RK, et al. Transcriptional control of preadipocyte determination by Zfp423. Nature. 2010; 464:619–623. [PubMed: 20200519]
13. Gupta RK, et al. Zfp423 expression identifies committed preadipocytes and localizes to adipose endothelial and perivascular cells. Cell Metab. 2012; 15:230–239. [PubMed: 22326224]
14. Tran KV, et al. The vascular endothelium of the adipose tissue gives rise to both white and brown fat cells. Cell Metab. 2012; 15:222–229. [PubMed: 22326223]
15. Wu J, et al. Beige adipocytes are a distinct type of thermogenic fat cell in mouse and human. Cell. 2012; 150:366–376. [PubMed: 22796012]
16. Lončar D. Convertible adipose tissue in mice. Cell Tissue Res. 1991; 266:149–161. [PubMed: 1747909]
17. Loncar D, Afzelius BA, Cannon B. Epididymal white adipose tissue after cold stress in rats. I. Nonmitochondrial changes. J Ultrastruct Mol Struct Res. 1988; 101:109–122. [PubMed: 3268608]
18. van Marken Lichtenbelt WD, et al. Cold-activated brown adipose tissue in healthy men. N Engl J Med. 2009; 360:1500–1508. [PubMed: 19357405]
19. Frontini A, Cinti S. Distribution and development of brown adipocytes in the murine and human adipose organ. Cell Metab. 2010; 11:253–256. [PubMed: 20374956]
20. Seale P, et al. PRDM16 controls a brown fat/skeletal muscle switch. Nature. 2008; 454:961–967. [PubMed: 18719582]
21. Lee YH, Petkova AP, Mottillo EP, Granneman JG. *In vivo* identifcation of bipotential adipocyte progenitors recruited by ^{2}3-adrenoceptor activation and high-fat feeding. Cell Metab. 2012; 15:480–491. [PubMed: 22482730]
22. Himms-Hagen J, et al. Multilocular fat cells in WAT of CL-316243–treated rats derive directly from white adipocytes. Am J Physiol Cell Physiol. 2000; 279:C670–C681. [PubMed: 10942717]
23. Granneman JG, Li P, Zhu Z, Lu Y. Metabolic and cellular plasticity in white adipose tissue I: effects of β3-adrenergic receptor activation. Am J Physiol Endocrinol Metab. 2005; 289:E608–E616. [PubMed: 15941787]
24. Barbatelli G, et al. The emergence of cold-induced brown adipocytes in mouse white fat depots is determined predominantly by white to brown adipocyte transdifferentiation. Am J Physiol Endocrinol Metab. 2010; 298:E1244–E1253. [PubMed: 20354155]
25. Birsoy K, et al. Analysis of gene networks in white adipose tissue development reveals a role for ETS2 in adipogenesis. Development. 2011; 138:4709–4719. [PubMed: 21989915]
26. Sun K, et al. Dichotomous effects of VEGF-A on adipose tissue dysfunction. Proc Natl Acad Sci USA. 2012; 109:5874–5879. [PubMed: 22451920]
27. Perl AKT, Wert SE, Nagy A, Lobe CG, Whitsett JA. Early restriction of peripheral and proximal cell lineages during formation of the lung. Proc Natl Acad Sci USA. 2002; 99:10482–10487. [PubMed: 12145322]

28. Soriano P. Generalized lacZ expression with the ROSA26 Cre reporter strain. Nat Genet. 1999; 21:70–71. [PubMed: 9916792]
29. Sharp LZ, et al. Human BAT possesses molecular signatures that resemble beige/brite cells. PLoS ONE. 2012; 7:e49452. [PubMed: 23166672]
30. Rosenwald M, Perdikari A, Rulicke T, Wolfrum C. Bi-directional interconversion of brite and white adipocytes. Nat Cell Biol. 2013; 15:659–667. [PubMed: 23624403]
31. Spalding KL, et al. Dynamics of fat cell turnover in humans. Nature. 2008; 453:783–787. [PubMed: 18454136]
32. Miller WH, Faust IM. Alterations in rat adipose tissue morphology induced by a low-temperature environment. Am J Physiol. 1982; 242:E93–E96. [PubMed: 7065129]
33. Gesta S, Tseng YH, Kahn CR. Developmental origin of fat: tracking obesity to its source. Cell. 2007; 131:242–256. [PubMed: 17956727]
34. Cartwright MJ, Tchkonia T, Kirkland JL. Aging in adipocytes: potential impact of inherent, depot-specific mechanisms. Exp Gerontol. 2007; 42:463–471. [PubMed: 17507194]
35. Macotela Y, et al. Intrinsic differences in adipocyte precursor cells from different white fat depots. Diabetes. 2012; 61:1691–1699. [PubMed: 22596050]
36. Tchkonia T, et al. Fat depot origin affects adipogenesis in primary cultured and cloned human preadipocytes. Am J Physiol Regul Integr Comp Physiol. 2002; 282:R1286–R1296. [PubMed: 11959668]
37. Baglioni S, et al. Functional differences in visceral and subcutaneous fat pads originate from differences in the adipose stem cell. PLoS ONE. 2012; 7:e36569. [PubMed: 22574183]
38. Vega GL, et al. Influence of body fat content and distribution on variation in metabolic risk. J Clin Endocrinol Metab. 2006; 91:4459–4466. [PubMed: 16926254]
39. Grundy SM, Adams-Huet B, Vega GL. Variable contributions of fat content and distribution to metabolic syndrome risk factors. Metab Syndr Relat Disord. 2008; 6:281–288. [PubMed: 18759660]

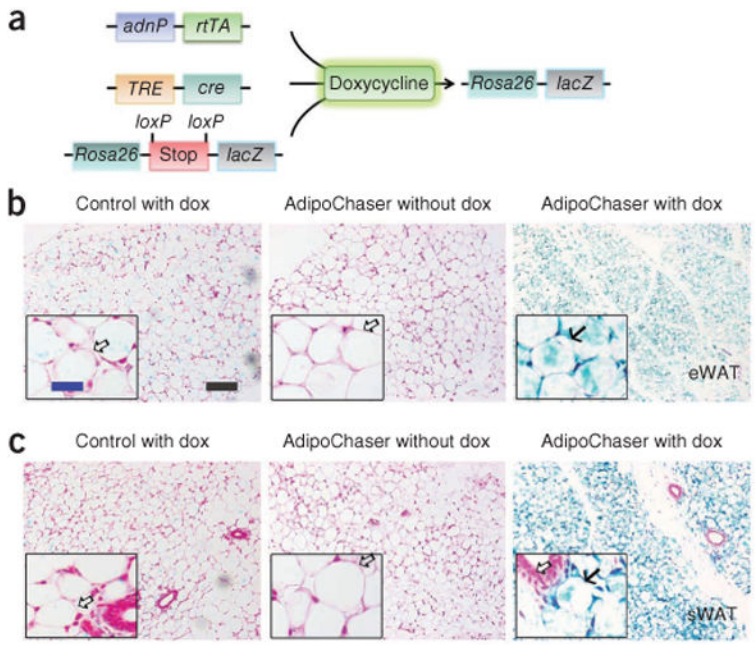

Figure 1.

Inducible labeling of mature adipocytes. (**a**) The inducible labeling system of mature adipocytes, produced by crossing *adiponectinP-rtTA* (*adnP-rtTA*) transgenic mice with *TRE-cre* and *Rosa26-loxP-stop-loxP-lacZ* transgenic mice. The triple transgenic mouse, called the AdipoChaser mouse, expresses rtTA in mature adipocytes but does not express LacZ in any cell type while maintained on food not containing doxycycline (dox). When doxycycline is included in the food, adipocytes that express rtTA will have the *TRE* promoter activated so that *cre* expression is induced. The Cre protein will specifically cut out the floxed transcriptional stop cassette and then turn on LacZ expression. Even after withdrawal of doxycycline from the food, these adipocytes will permanently express LacZ, whereas any new adipocytes that develop after doxycycline exposure will not express LacZ. (**b,c**) Representative β-gal (blue) staining of eWAT (**b**) and sWAT (**c**) in male control (mice with only *TRE-cre* and *Rosa26-loxP-stop-loxP-lacZ)* or AdipoChaser mice. Solid arrows (**b,c**), LacZ-positive cells; open arrows (**b,c**), LacZ-negative cells. Scale bar (black, shown in **b**, applies to **b** and **c**), 200 μm; (blue, shown in **b**, applies to the insets in **b** and **c**), 50 μm. Throughout the figure, $n = 2$ male mice per group.

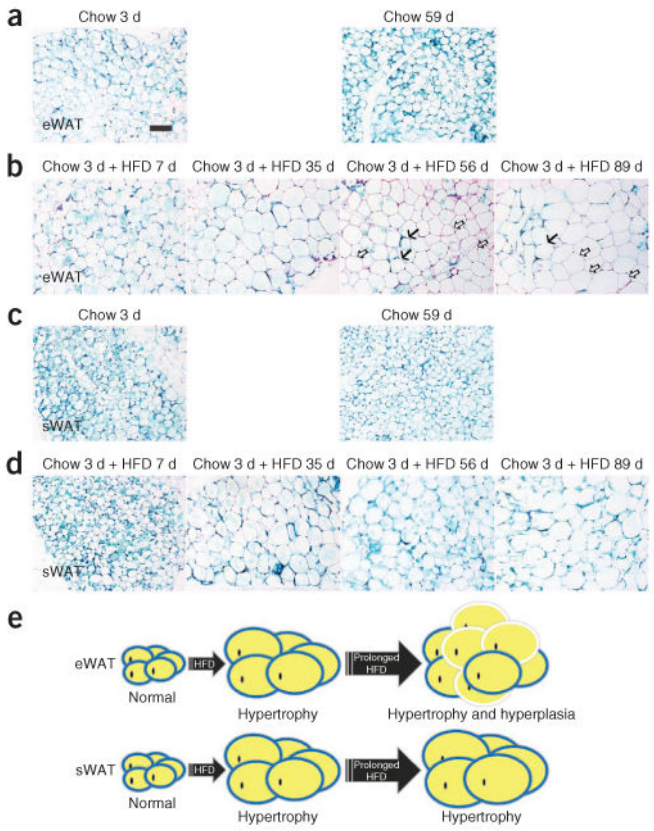

Figure 2.

HFD-induced adipose tissue hypertrophy and hyperplasia. (**a–d**) Representative β-gal staining of eWAT (**a,b**) and sWAT (**c,d**) from 9- to 10-week-old male AdipoChaser mice that were kept on doxycycline diet for 7 d followed by chow diet for 3 or 59 d (**a,c**) or chow diet for 3 d and HFD for 7, 35, 56 or 89 d (**b,d**). Solid arrows (**b**), LacZ-positive cells; open arrows (**b**), LacZ-negative cells. Scale bar (shown in a, applies to **a–d**), 200 μm. For **a–d**, *n* = 3 male mice per group. (**e**) Schematic model of the depot-dependent contribution of hyperplasia to adipose tissue expansion after HFD feeding. HFD-induced adipose tissue expansion is contributed mainly by hypertrophy in both eWAT and sWAT at the early stages. After prolonged HFD exposure (i.e., longer than 1 month), a wave of adipogenesis is preferentially initiated in eWAT (hyperplasia), but adipogenesis does not occur at measurable levels in sWAT. Adipocytes surrounded by blue circles represent old LacZ-positive cells, and adipocytes surrounded by white circles represent new LacZ-negative cells.

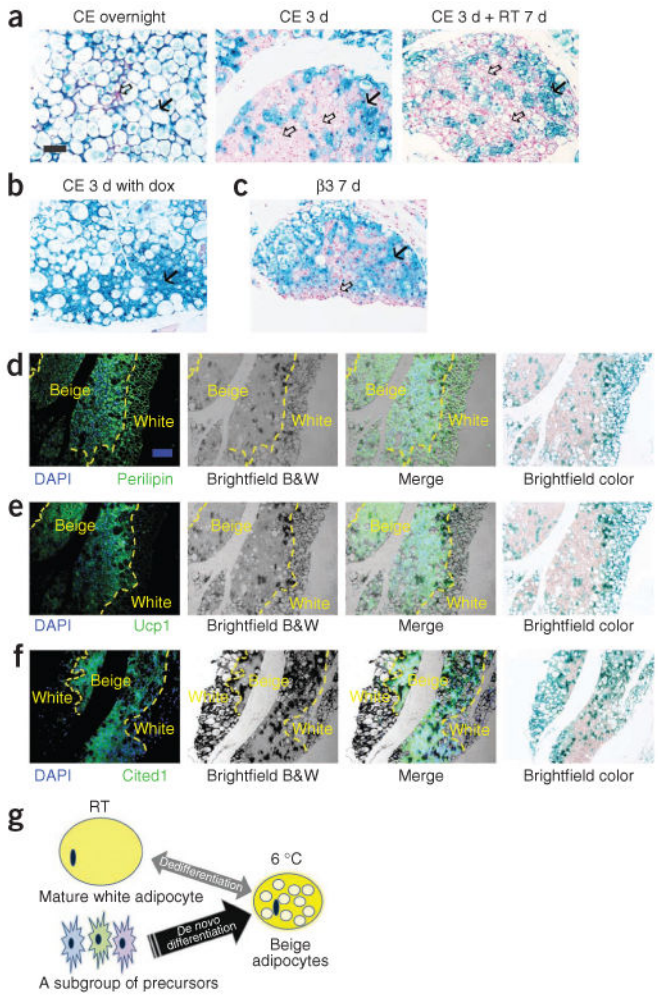

Figure 3.

Lineage of the brown-like adipocytes in subcutaneous adipose tissue after cold exposure. (**a**) Representative β-gal staining of sWAT from 10-week-old male AdipoChaser mice that were kept on doxycycline diet for 7 d followed by chow diet for 3 d and then exposed to cold (CE) overnight (left) or for 3 d (middle) or exposed to cold for 3 d followed by 7 d in room temperature (RT; right). (**b**) Representative β-gal staining of sWAT from 10-week-old male AdipoChaser mice that were on doxycycline diet before and during 3 d of cold exposure as a positive control group. (**c**) Representative β-gal staining of sWAT from 10-week-old male AdipoChaser mice on doxycycline diet for 7 d followed by chow diet for 3 d and then given 7 d of daily β3 agonist treatment. Solid arrows (**a–c**), LacZ-positive cells; open arrows (**a,c**), LacZ-negative cells. Scale bar (shown in a, applies to **a–c**), 100 μm. For **a–c**, *n* = 3 male mice per group. (**d–f**) Immunofluorescence staining for perilipin (green) (**d**), Ucp1 protein (green) (**e**) or Cited1 protein (green) (**f**) on slides prestained with β-gal. The male AdipoChaser mice in d–f were pretreated with doxycycline diet and exposed to cold for 3 d on a chow diet. Blue indicates pre-existing white adipocytes. Scale bar (shown in **d**, applies to **d–f**), 200 μm. The yellow dashed outlines indicate the borders between white and beige adipocytes. For **d–f**, *n* = 2 male mice per group. B&W, black and white. (**g**) Schematic

model showing that the beige cell population arises predominantly from *de novo* adipogenesis rather than transdifferentiation. After cold exposure or β3 agonist treatment, most beige adipocytes are induced by differentiating from cell populations other than existing mature adipocytes (beige precursors) rather than through dedifferentiation of mature white adipocytes.

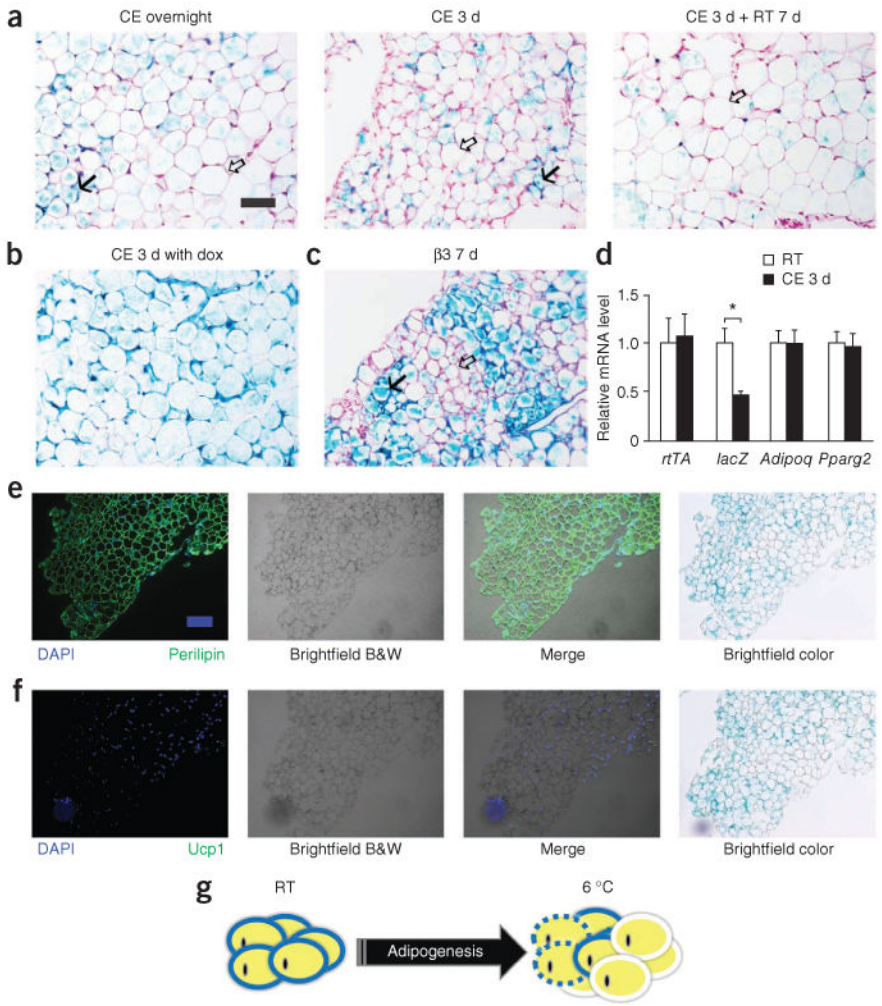

Figure 4.

Adipogenesis in epididymal adipose tissue during cold exposure. (**a**) Representative β-gal staining of eWAT from AdipoChaser mice after overnight (left) or 3 d of cold exposure (middle) or 3 d of cold exposure followed by 7 d in room temperature (right). (**b**) Representative β-gal staining of eWAT from male AdipoChaser mice that were on doxycycline diet before and during 3 d of cold exposure as a positive control group. (**c**) Representative β-gal staining of eWAT from AdipoChaser mice after 7 d of daily β3 agonist treatment. Solid arrows (**a,c**), LacZ-positive cells; open arrows (**a,c**), LacZ-negative cells. Scale bar (shown in **a**, applies to **a–c**), 100 μm. For **a–c**, *n* = 3 male mice per group. (**d**) Relative mRNA expression levels of *rtTA, lacZ, Adipoq* and *Pparg2* in eWAT from mice at room temperature or exposed to cold for 3 d. *Gapdh* was used as an endogenous control. *n* = 11 male mice per group. Data are shown as the mean ± s.e.m. **P* = 0.003 by unpaired two-tailed *t* test compared to the room temperature group. (**e,f**) Immunofluorescence staining for perilipin (green) (**e**) and Ucp1 protein (green) (**f**) on slides prestained with β-gal. The male AdipoChaser mice in e and f were pretreated with doxycycline diet and exposed to cold for 3 d on a chow diet. Scale bar (shown in **e**, applies to **e** and **f**), 200 μm. (**g**) Schematic model of *de novo* adipogenesis of white adipocytes in eWAT during cold exposure or β3 agonist

treatment. Unlike sWAT, eWAT responds to cold or β3 agonist treatment by initiating massive adipogenesis. Adipocytes surrounded by blue circles represent old LacZ-positive cells, adipocytes surrounded by white circles represent new LacZ-negative cells, and adipocytes surrounded by dashed blue circles represent potential adipocyte death.

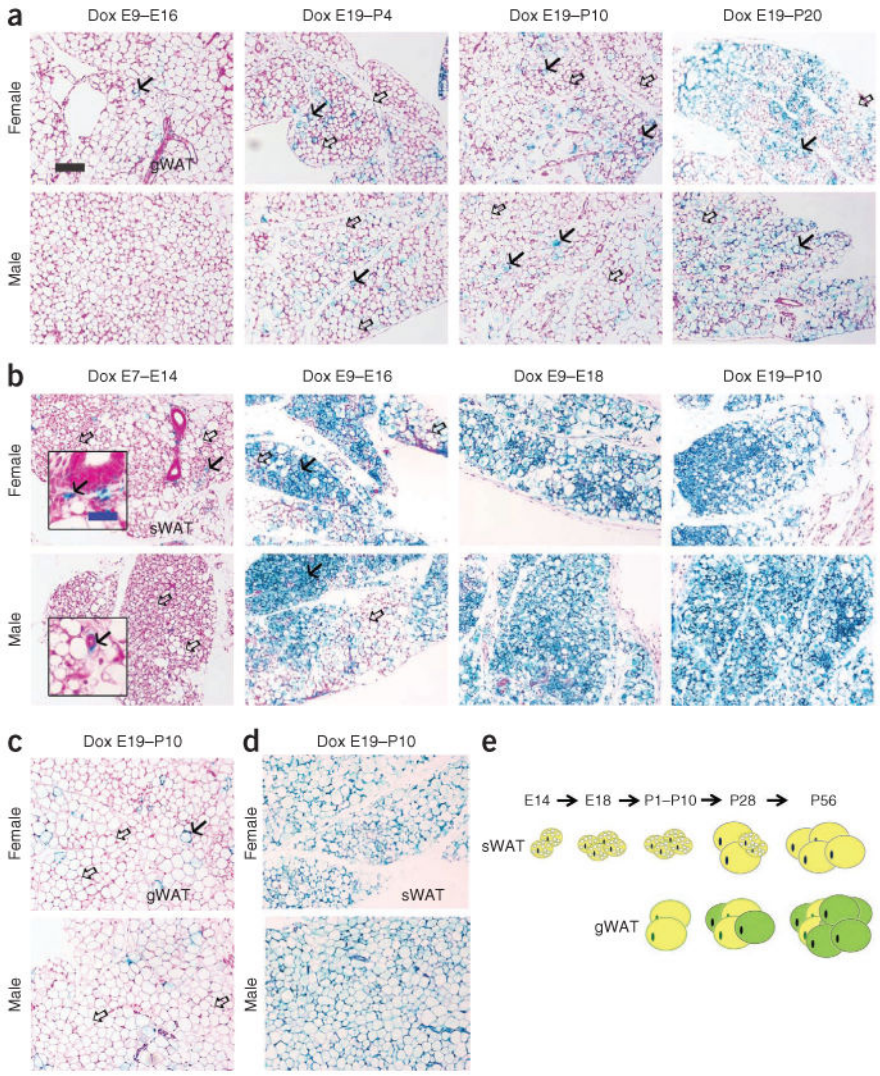

Figure 5.

Development of epididymal and subcutaneous adipocytes during embryonic and postnatal development. (**a-d**) Results from AdipoChaser mice that were on doxycycline diet for the indicated number of days during embryonic and postnatal development that were thereafter kept on chow diet. (**a**) Representative β-gal staining of gonadal WAT (gWAT) from 28-day-old female mice (top) and male littermates (bottom). The mothers of these mice were on doxycycline diet during E9-E16, E19-P4, E19-P10 or E19-P20, as indicated. (**b**) Representative β-gal staining of sWAT from 28 day-old-female (top) and male (bottom) mice. The mothers of these mice were on doxycycline diet during E7-E14, E9-E16, E9-E18 or E19-P10, as indicated. (**c,d**) Representative (3-gal staining of gWAT of 56-day-old female (**c**, top) and male (**c**, bottom) mice and of sWAT from 56-day-old female (**d**, top) and male (**d**, bottom) mice. The mothers of these mice were on doxycycline diet during E19-P10. Solid arrows (**a–c**), LacZ-positive cells; open arrows (**a–c**), LacZ-negative cells. Scale bar (black, shown in **a**, applies to **a–d**). 200 μm; (blue, shown in **b**, applies to the insets in **b**), 50 μm. For **a–d**, *n* = 2 mice per group. (**e**) Schematic model of the development of

gWAT and sWAT. Adipocytes in the gWAT are differentiated postnatally between birth and sexual maturation, whereas all the adipocytes in the subcutaneous adipose tissue start to differentiate between E14 and E18, but the differentiation takes much longer and finishes postnatally. Yellow adipocytes represent adipocytes differentiated before birth, and green adipocytes represent adipocytes differentiated postnatally.